Soft Matter

Accepted Manuscript

ROYAL SOCIETY OF CHEMISTRY

www.rsc.org/softmatter

TOC

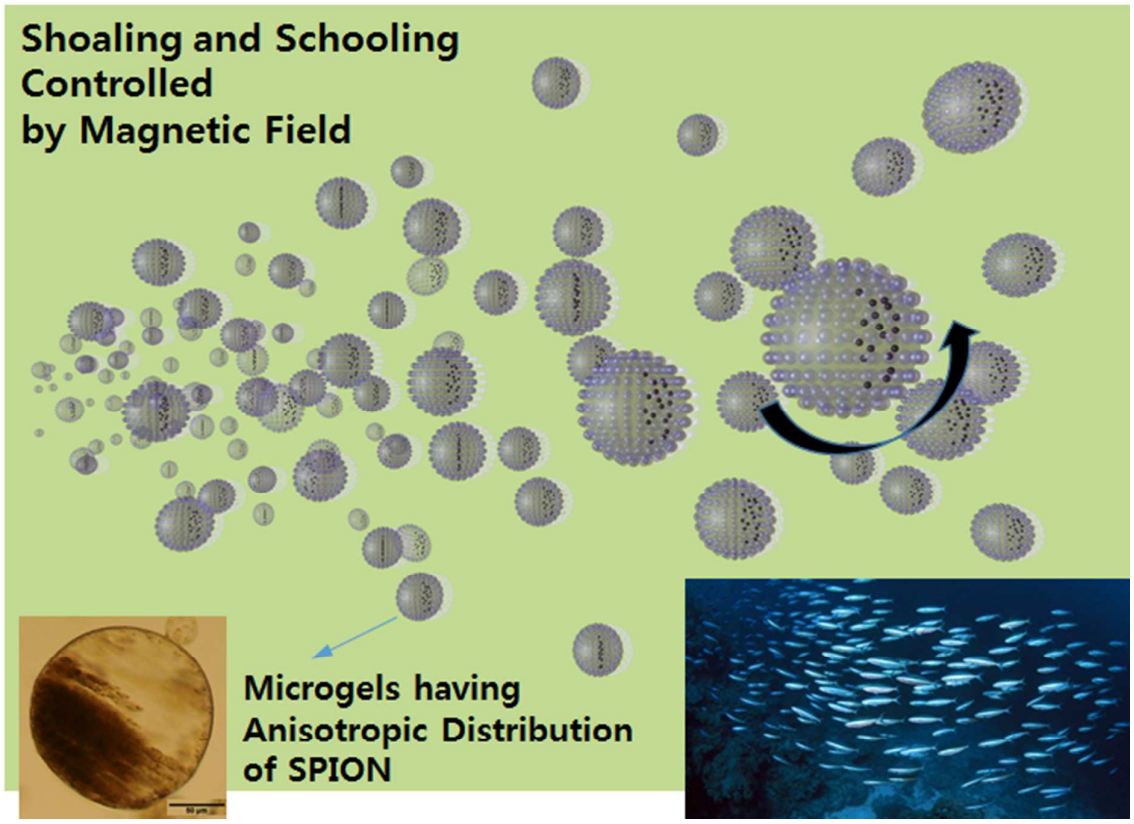

A novel technique of unrestricted flow control was developed using microgels with an anisotropic distribution of SPIONs, biomimicking the flow generated by a school of fish.

Translational and rotational motion control of microgels enabling shoaling and schooling

You-Jin Kim and Jonghwi Lee*

Department of Chemical Engineering and Materials Science, Chung-Ang University, 221, Heukseok-dong, Dongjak-gu, Seoul, 156-756, Republic of Korea

E-mail: jong@cau.ac.kr

A technique for adequate flow control is important in the fields of science and engineering. In this study, we hypothesized that the unrestricted flow control inside a chamber containing 'schools of magnetic particles' might be possible through control of an external magnetic field, biomimicking the flow generated by schools of fish. Microgels based on superparamagnetic iron oxide nanoparticles (SPIONs) and poly(acrylic acid) hydrogels were employed. With an increase in the SPION content, the microgels responded more efficiently to the translational movement of the magnetic field. Rotational movement was more efficiently achieved with anisotropic distribution of SPIONs inside microgels, which was induced by applying magnetic field immediately prior to crosslinking. The systems of the anisotropic microgels successfully provided microflow for effective mixing in a capillary. This biomimetic flow control may be useful for the control of fluid systems of any micro or nano size and any shape, regardless of the tortuosity.

1. Introduction

In nature, fish group together, a behavior known as shoaling, for various reasons, and they move in a coordinated manner, which is termed schooling.[1] This behavior has distinct social advantages as well as other advantages such as avoiding predation and improving foraging.[2] Among the reasons, one major driving force for group formation is increased hydrodynamic efficiency. Fish use surrounding vortices produced by the movement of other fish to reduce energy exertion through the adjustment of their bodies.[3,4] Slaloming motions allow them to push off the vortices and maneuver between them. However, coordinated group movement creates a large flux, which increases predator detection in certain conditions, a disadvantage of shoaling and schooling.[1] Thus, certain species has active shoaling and schooling patterns only during the day and stop shoaling and reduce their swimming speed at night.[5]

Shoaling and schooling phenomena could be utilized as a novel biomimetic strategy for mixing and fluid transport. If the translational and rotational movements of numerous particles are arbitrarily controlled, a controllable flow useful in any fluid chamber can be created, which has never been achieved by conventional stirring with predetermined patterns. Flow control via a 'school of particles' is not limited to the size or shape of the chamber. For example, if sufficiently small particles are used, fluids in any tortuous small chamber can be effectively stirred.

The translational and rotational motions of many-particle systems can be controlled by an external magnetic field if the particles are superparamagnetic. By arbitrarily moving a magnet on the outside of a fluid chamber, particles undergoing any type of motion other than circular can be controlled. Furthermore, the particles can conveniently be separated from the reaction medium by application of a magnetic field. The isotropy of the structure of superparamagnetic domains within a particle will influence the responsive behaviors of many particles. For example, spherical superparamagnetic iron oxide nanoparticles (SPIONs) may

not effectively respond to a rotational magnetic field. Therefore, magnetic field-responsive microgels were investigated in here with isotropic or anisotropic distributions of SPIONs for use as a novel flow generation tool.

If microgel particles efficiently respond to a moving external magnetic field, the microgels can be used to mix materials within microfluidic units, which is an important issue in labs-on-a-chip.[6,7] Microscale mixing in microfluidic systems is crucial for successful application performance such as DNA hybridization and PCR amplification.[8,9] Among the mechanisms of mixing, i.e., bulk diffusion, eddy diffusion, and molecular diffusion, molecular diffusion becomes more dominant when the channel dimension decreases to micron size.[10,11] However, molecular diffusion is limited even though an increased interfacial area is used. Passive mixing using a static mixer and active mixing using micromachined stirrers have also been developed.[10] Well-positioned micromachined magnetic bars, several hundreds of microns in size, for lab-on-a-chip applications[12] and artificial cilia based on the electroactuators of polymer fibers have been examined.[13] However, the development of microscale mixing has lagged behind the rapid development of micro- and nano-fluidics.[14]

Magnetic microgels have been developed for primarily attracting molecules and cells for detection, catalysis, or other purposes, utilizing the separation advantage that they can be removed by a magnetic field.[15-17] Magnetic microgels are typically prepared by dispersing SPIONs in a hydrogel matrix.[18] The hydrogel matrix prevents aggregation issues. Only a few studies have reported on the motion control of the SPION-containing particles.[19] Siegel et al. showed that a system of superparamagnetic particles was developed for alternating movement between surfaces through the application of electromagnets on both surfaces.[19] Yang reported the motion control of Janus microgels with SPIONs that produced translational and rotational motion control through the application of an external magnetic field.[20] The microgels were prepared by a simple emulsion method. However, no further studies on flow

control or the role of anisotropy in motion control have been reported.

Herein, a school of microgels with anisotropic distribution of SPIONs was investigated as a novel flow generation tool. The distribution of SPIONs inside the microgels was organized to be anisotropic through application of an external magnetic field and was immobilized by subsequent chemical crosslinking. The role of anisotropy in motion control efficiency was investigated. For flow control in real applications, the size of the particle was critical as it determines the size of the generated vortex, particle drag force, etc. Thus, a responsive hydrogel of poly(acrylic acid) (PAA) was developed herein as the matrix of the microgels, and its responsive size variation was systematically investigated.

2. Materials and method

Acrylic acid (99%), 2,2'-azobis(2-methylpropionamidine) dihydrochloride (V-50), *N,N'*-methylenebisacrylamide (MBA), iron (III) chloride hexahydrate ($FeCl_3 \cdot 6H_2O$, 97%), dimethyldichlorosilane, rodamine-B, and iron (II) chloride tetrahydrate ($FeCl_2 \cdot 4H_2O$, 99%) were purchased from Sigma-Aldrich (MO, USA). Silica nanoparticles (SiO_2, average diameter 40 nm, Aerosil TT600, Evonik, Korea), toluene (Duksan, Korea), methanol (Duksan, Korea), 2-propanol (Duksan, Korea), double-distilled water (Duksan, Korea), phosphate buffer solutions (SamChun, Korea, pH 2, 7 and 9, 10 mM), and ammonia water (25 – 30%, Duksan, Korea) were used without purification.

$FeCl_3 \cdot 6H_2O$ (0.5 g) and $FeCl_2 \cdot 4H_2O$ (0.25 g) were sequentially dissolved in 2-propanol (50 mL) under a nitrogen atmosphere at RT. After heating to 80 °C, an excess of ammonia water (10 mL) was mixed for 15 min under stirring, followed by cooling in a 5 °C chamber for 5 hrs. The supernatant was removed while a neodymium magnet (15 x 40 x 10 mm) held SPIONs to the bottom of reactor. After injecting 50 mL methanol and vortexing for

1 min, the solution was centrifuged at 10000 rpm for 5 min (Mega 17R, Hanil, Korea) to remove residual reactants. This purification step was repeated three times. As the final step, the SPIONs were homogeneously dispersed in water using an ultrasonicator (VCX-750, SONICS, USA) (Fig. S1).

For the preparation of hydrophobic nanoparticles, SiO_2 nanoparticles (1 g), which were initially hydrophilic, were homogeneously dispersed in distilled water (10 mL) and mixed with dimethyldichlorosilane (0.1 mL) for 5 min under stirring. The solution was dried in an 80 °C convection oven for 24 hrs, and the resulting powder was used for further analysis (Fig. S1).

A water phase was prepared by adding acrylic acid (10 wt%), V-50 (1/5 of monomer weight), and MBA (1/5 of monomer weight) into the SPION water dispersion (0.363, 0.725, 1.45 wt%; 1.45 wt% unless otherwise stated). A continuous oil phase was prepared by dispersing the hydrophobic SiO_2 nanoparticles (10 wt%) into toluene using an ultrasonicator (VCX-750, SONICS, USA) for 3 min (10 sec running time and 10 sec rest). The water and oil phases (1:3 vol. ratio) were emulsified in a vial under mechanical stirring at 1000 rpm (HT-50DX, Wisestir, Korea) for 30 min. After mixing, a neodymium magnet (15 x 40 x 10 mm) was attached to the sidewall of the vial to induce anisotropic distribution of SPIONs in the water phase. The long axis of the magnet was parallel to the long axis of the vial. The sample was then placed in an 80 °C oven (OF-02GW, JEIO Tech, Korea) for thermal crosslinking for 6 hrs. Isotropic microgels were prepared following the same procedure without a magnet. After crosslinking, microgels were washed three times with 20 mL acetone over a 100 μm sieve and dispersed in water.

Nanoparticles dispersed in water were collected on a copper grid and examined by transmission electron microscopy (TEM, JEM-2100F, JEOL, USA). Microgels were examined by optical microscopy (OM, BX-51, Olympus, Japan) and scanning electron

microscopy (SEM, S-3400N, Hitachi, Japan, 10 kV). For SEM, microgels were frozen in liquid nitrogen and freeze dried (FD-1000, EYELA, JAPAN) for 24 hrs. The dried particles were mounted on a carbon tape and coated with Pt by a sputter coater (E-1010, Hitachi, Japan) for 120 sec at 15 mA. The size of the microgels was analyzed in distilled water (150 mL) by a particle size analyzer (HORIBA, LA-910, Japan, 632.8 nm He-Ne laser, 1.2 ± 0.00i relative refractive index) without sonication.

The translational velocity was measured by applying a magnetic field (neodymium magnet 15 x 40 x 10 mm) 20 mm from the position of the microgels, and the time needed for the microgels to move 10 mm was measured. The microgel concentration was 10 wt%, and a Teflon container of 20 x 10 x 2 mm was used. The rotational velocity was assessed using the same microgel dispersions and container using a charge coupled device (CCD) recording of the optical microscope (Software: Tomoro). A rotational magnetic field was applied by a magnetic stirrer (SG.285416373, Schott, USA) to capillary tubes (HCH-41A2502, Chase, USA, I.D. 1.15 mm) placed in a Teflon container (1000 rpm, for 24 hrs). The average values of both the translational and rotational velocities were obtained from three repeated tests.

3. Results and Discussion

A. Preparation of anisotropic microgels

Anisotropic distribution of SPIONs in the water phase was induced by a magnetic field and was subsequently immobilized by crosslinking (Fig. 1). SPION particles easily aligned with the magnetic field. The sufficient SPION response speed to the magnetic field prevented any problems related to competition between the alignment rate and the crosslinking rate. Instead, the role of the Pickering emulsion was important.[21] The silica nanoparticles were able to prevent the migration of SPIONs into the oil phase, particularly during magnetic alignment.

Furthermore, they provided enough emulsion stability to prevent aggregation between the colloidal particles.

Particle movement of microgels by thermal vibration interfered with the anisotropic alignment of SPIONs due to the external magnetic field, but the size of the microgels was large enough to reduce the thermal vibration. The viscosity of the water phase was also sufficient to fix the alignment of SPION nanoparticles before crosslinking resulted in gelation. As a result, no significant random diffusion of SPION nanoparticles was noticed after their alignment.

After crosslinking, the successful preparation of anisotropic microgels was verified by OM (Fig. 2). The fraction of SPIONs in the microgels was 5 wt%, and they produced ca. 1/3 of whole spheres dark (opaque). The preparation method was quite simple and straightforward. Depending on the scale of the magnetic field, large-scale preparations will be readily achieved. As a control, isotropic microgels were also prepared (Fig. 2). The isotropic microgels showed some density fluctuation of the SPIONs but did not show any directional dependency. The low degree of inhomogeneity in local SPION density seemed to develop by increased viscosity and local temperature fluctuation due to the crosslinking reaction.[22, 23]

Under SEM, the microgel particles showed rough surfaces (Fig. 3), which were freeze-dried after rapid freezing in liquid nitrogen. The hydrogel materials of PAA are intrinsically porous.[24] Thus, the rough texture was posited to originate from the shell layers of silica nanoparticles over the porous PAA. The magnified image of Fig. 3 suggests that the shell layer of silica nanoparticles produced by Pickering emulsion is not a perfect monolayer.

B. Shoaling and schooling

Upon applying a magnetic field, microgels were attracted to the magnet, and particle translational velocity was measured (Fig. 4). The group movement of microgels depends on

various parameters; by maintaining other parameters constant, the SPION content inside the microgels (concentration of SPION solution) was systematically changed, as shown in Fig. 4. As a result, the translation velocity appeared to linearly depend on the SPION content. The SPION particles responded to the external magnetic field and generated force for linear movement of the microgels. The speed achieved with an increased SPION content was more than one order of magnitude faster than that previously reported in artificial cilia.[13]

Small magnetic particles typically less than 1 μm produced interesting magnetic fluid behavior such as magnetorheology.[25] In the cases of relatively large particles greater than 1 μm, magnetophoresis is the typical phenomenon, which is based on simple translational motion control by a gradient force along the gradient of the magnetic field.[25] The force acting on a particle, F_m, in a fluid with mismatching susceptibilities is

$$F_m = \frac{V(\chi_p - \chi_f)}{\mu_0}(B \cdot \nabla)B$$

where V is the volume of the particle, B is the flux density, χ is the susceptibility of the particle or fluid, and μ_0 is the permeability of the vacuum.

When a microgel reaches a steady speed movement, which appeared to be achieved easily in this experiment, the induced magnetic force, F_m, should be balanced with the particle drag force, F_D, which is

$$F_D = 0.5\rho v^2 C_D A$$

where ρ is the density of the fluid, υ is the relative speed of the microgels, A is the cross-sectional area, and C_D is the drag coefficient (dimensionless number).[26] The diameters of the 1.45, 0.725, and 0.363 wt% microgels were 269, 174, and 133 μm, respectively (Fig. 7). Compared to the drag force of the 0.363 wt% microgel, $F_D(0.363)$, that of the 0.725 wt% sample, $F_D(0.725)$, was $2.8F_D(0.363)$, if the above equation was employed. With a further increase in the SPION content, $F_D(1.45)$ was $13.1F_D(0.363)$. Therefore, the drag force

predicted increased more rapidly with an increase in the content of the SPION compared to the linear relationship shown in Fig. 4. Of course, the equation cannot precisely explain the effects of the SPION content as C_D is considered a constant and the different types of drag modes and inter-particle interactions were neglected.

Translational and rotational motions were controlled for the anisotropic microgels. Fig. 5 shows the effect of anisotropy. As a control, microgels without SPIONs were compared and showed no response to an external magnetic field. With the addition of SPIONs into microgels, a response to the rotational external magnetic field was obvious. Although the content of the SPIONs was maintained, the rotational velocity dramatically increased with anisotropic alignment. The rotational velocity of anisotropic microgels was 4.2 times greater than that of the isotropic microgels. Therefore, for effective control of the translational and rotational motions, anisotropic distribution of SPIONs is necessary. Our preparation method will allow anisotropic microgels to be prepared in a large quantity and many-particle systems can be constructed to mimic the shoaling and schooling of fish.

Fig. 6 shows the rotational motion induced in a microcapillary. Numerous microgels inside the microcapillary can be rotated and generated microscale mixing effects (SI). The microgels were located in the middle, separating one side of the microcapillary filled with red dye solution and another filled with pure water. When a rotational magnetic field was applied to the systems of anisotropic microgels (Fig. 6a and 6d), isotropic microgels (Fig. 6b and 6e), and the system without microgels (Fig. 6c and 6f), relatively fast diffusion of the dye solution was observed in the anisotropic microgels, which is quite distinct from the other two cases. No significant difference in diffusion was identified between the isotropic microgels and the system without microgels. In our observation on the group motion of microgels, isotropic microgels cannot produce a harmonic motion to create effective convection microflow in the capillary. The existence of microgels itself simply blocks the diffusion of dye, instead. The

insufficient convection by the response of isotropic microgels to the rotational magnetic field seems to be unable to overcome the diffusion barrier effect of microgels. As a result, its diffusion rate becomes similar to the simple diffusion rate of the no-microgel case, which is driven by only the concentration gradient.

This simple experiment shows that the anisotropic distribution of SPIONs is important for the effective response of microgels to a rotational magnetic field. These microgels can be used as 'micro-stirrers' for microfluidic devices or any other micro-systems.

C. Responsive change of the particle size

The particle size is a critical parameter in determining the drag force, which determines the movement of microgels. Therefore, the particle size change offers an *in-situ* parameter to control the speed of translational and rotational motions. The PAA of microgels is responsive to pH: the volume expands (swells) with an increase in pH due to the strong charge-charge repulsion between acrylic acids through deprotonation.[27] Fig. 7 illustrates the particle size distributions of microgels in water and pH buffers, where the pH-dependent volume change of PAA is distinct. At a constant SPION concentration, the particle size of the microgels increased with an increase in pH.

With the addition of pH buffer into pure water, the ionic strength increased and the charge-charge repulsion between the carboxylic acids of PAA was screened. Therefore, volume shrinkage of microgels is expected upon the addition of buffer agents, as confirmed in Fig. 7. Both cases of pH 2 and 7 showed smaller particle sizes than the cases of water. As a result, the particle sizes of microgels in Fig. 7 indicate that size can be conveniently varied from 60 to 300 μm depending on the pH and ionic strength, without changing the degree of crosslinking or the initial preparation conditions of the microgels.

While the effects of the medium were quite predictable, the effect of the SPION

content was not. The particle size increased with an increase in SPION content in water, but the trend was opposite in pH 2 buffer solution: a lower SPION content resulted in a larger size. The same trend was found in the cases of pH 7 (Fig. 7). The 0.36 wt% microgels, the lowest content, showed the smallest particle size in water but the largest particle size in pH 2 and 7 buffers. The volume transition of microgels was more dramatic with an increase in SPION content.

There is a charge-charge repulsion contribution from the SPIONs. The charge-charge repulsion exists between the carboxylic acids of PAA, between the carboxylic acids of PAA and the surface functional groups of SPION, and between the surface functional groups themselves, which were screened using the same mechanism as for the buffer ions. Therefore, with increasing SPION content, a more significant volume transition due to the changes in ionic strength or pH was expected.

The strong interactions between the carboxylic acids of PAA and the polar functional groups on the surfaces of SPIONs[28,29] can be used to modify the surfaces of SPIONs or further conjugation with other molecules. Thus, SPIONs can act as crosslinkers in microgels.[30,31] With an increase in SPION content, the degree of crosslinking increased. However, with the addition of a buffer solution of pH 7, the strong charge-charge interactions were screened, resulting in large volume shrinkage of the 1.45 wt% microgel cases, from 300 μm to 90 μm. Similarly, this screening effect induced further volume shrinkage with a decrease in pH from 7 to 2. Alternatively, there was a small influence of the polar functional groups of SPION in the cases of 0.36 wt%. Thus, there were relatively small changes in volume in the 0.36 wt% case with the addition of buffer agents or a decrease in pH, resulting in opposite trends of the effects of SPION content.

Then, why does the particle size increase with an increase in SPION content in water? This relation seems to result from the preparation conditions. The initial particle

sizes of microgels in water are determined directly from the preparation conditions. Indeed, before crosslinking, the initial sizes of the water phase in oil continuous medium were dependent on the SPION content. Although we used the same experimental conditions for all three microgels, the different SPION contents produced different viscosities in the water phase. With an increase in SPION content, larger water droplets were formed in the oil phases due to the high viscosity, which determined the initial particle sizes of microgels in water after crosslinking. It was markedly noticed in our experiment the increase of the solution viscosity with an increase in SPION concentration, which is a characteristic property of nanoparticle dispersions.

There are several possible weaker effects of the nanoparticles. Silica nanoparticles can provide a hard shell to PAA microgels, which can hinder the volume transition of PAA via the high modulus of the shell. Similarly, SPION can act as a strengthening filler to increase modulus and hinder the volume transition of PAA. Higher interactions between SPION and PAA will hinder the volume transition via more effective load transfer from the hydrogel matrix to the fillers. If this is significant, swelling and deswelling will induce a particle shape change in anisotropic microgels from spherical to nonsymmetrical (distorted elliptical). However, the counteracting charge-charge repulsion effect from the incorporation of SPIONs increases the sensitivity of SPION-containing PAA to buffer agents and pH. Overall, the reduction of strength of the nanofillers was marginal. When a single anisotropic particle was observed under pH changes, no significant symmetry change was noticed (Fig. S3). The whole particle volume was sensitive to pH, but the SPION-concentrated compartment did not show a distinct difference in volume transition compared to the other compartment without SPIONs. Only the hindrance effect of silica nanoparticles was significant as the volume transition of the 0.36 wt% cases was relatively small compared to that of PAA.

4. Conclusions

Novel microgels were developed to induce local flux through translational and rotational motion control in many-particle systems, which mimic the 'shoaling and schooling' of fish. The microgels contained anisotropically-distributed SPIONs, allowing them to effectively respond to the translational and rotational inductions of an external magnetic field. The velocity of the translational motion was linearly proportional to the content of SPION in the microgels. The velocity of the rotational motion was distinctly fast compared to the cases with isotropically-distributed SPIONs or no SPIONs. Thus, these microgels can be used as effective microstirrers in a microcapillary. The preparation technique of the novel microgels is based on simple Pickering emulsion, allowing easy large-scale production. These anisotropic microgels present the possibility of new microflow control and related applications.

Acknowledgements

This work was supported by a National Research Foundation grant funded by the Korean Ministry of Science, ICT and Future Planning (NRF-2013R1A1A2021573 & Engineering Research Center of Excellence Program No. 2014R1A5A1009799).

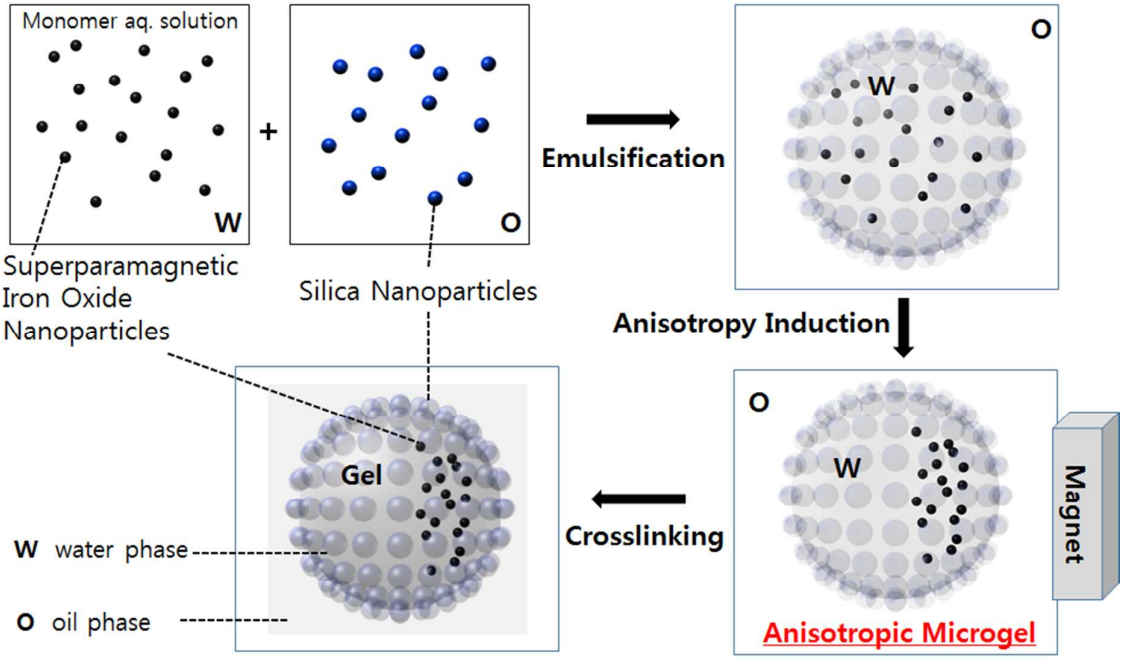

Fig. 1 Preparation of Pickering emulsion and superparamagnetic anisotropic microgels.

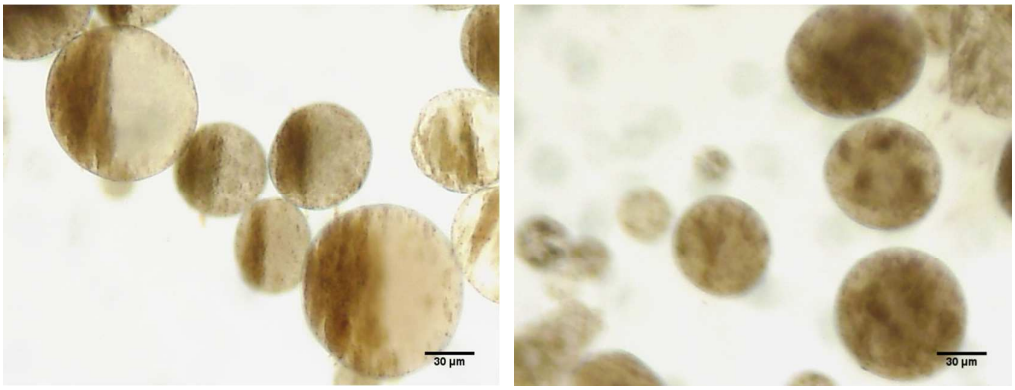

Fig. 2 Optical microscopic images showing the internal distribution of SPIONs: anisotropic microgels (left) and isotropic microgels (right).

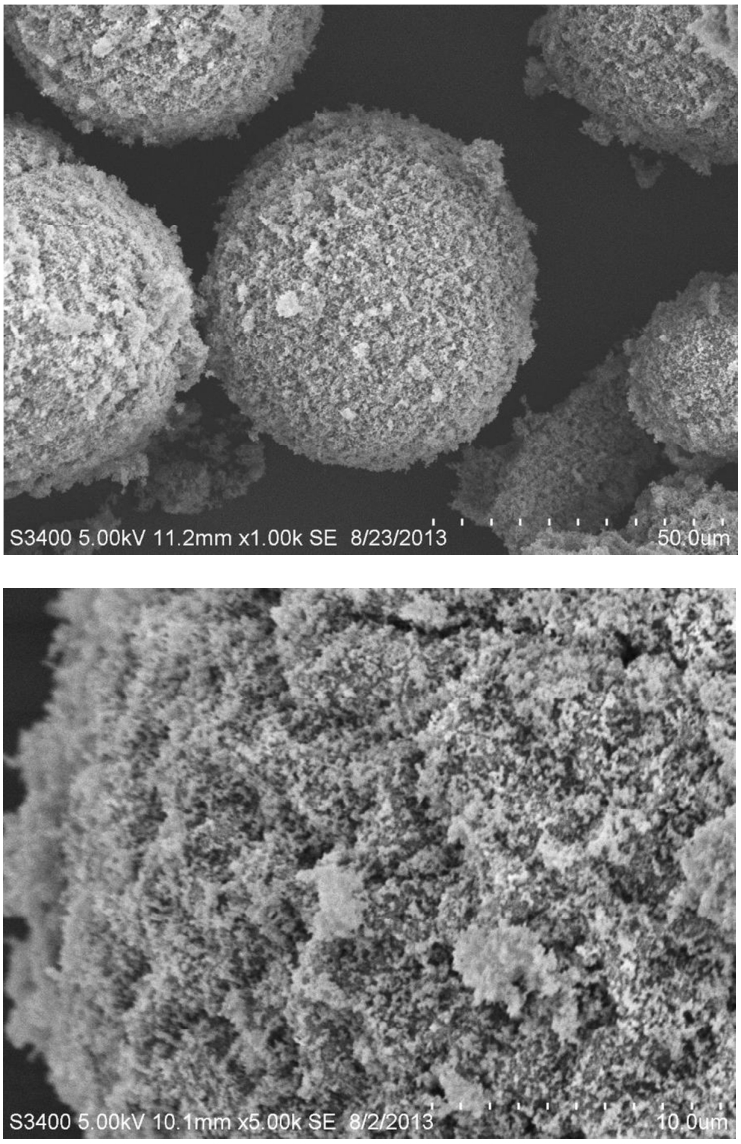

Fig. 3 SEM images of anisotropic microgels containing SPIONs.

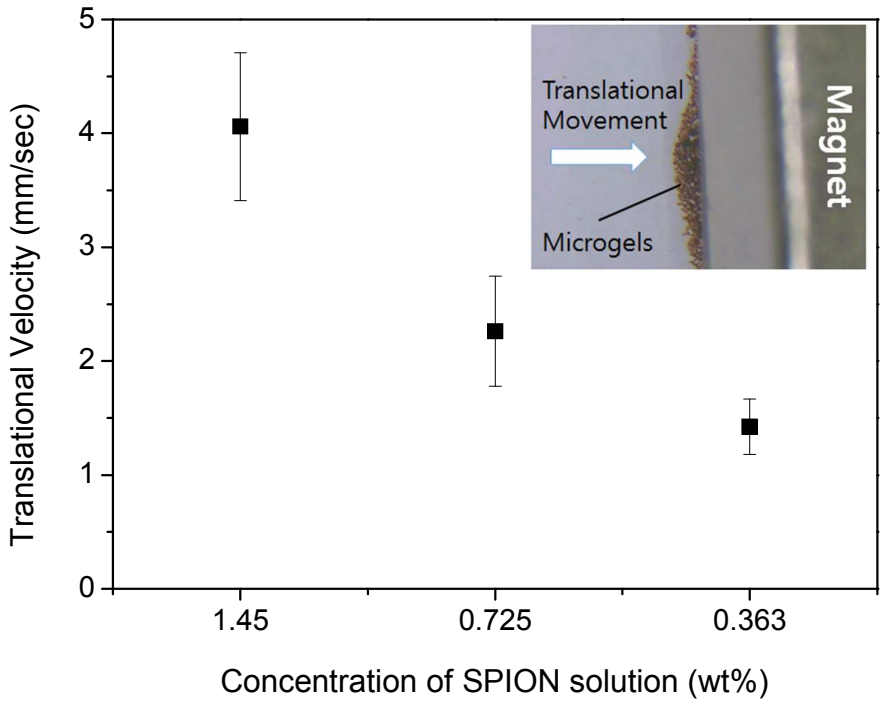

Fig. 4 Translational velocity of anisotropic microgels as a function of SPION concentration.

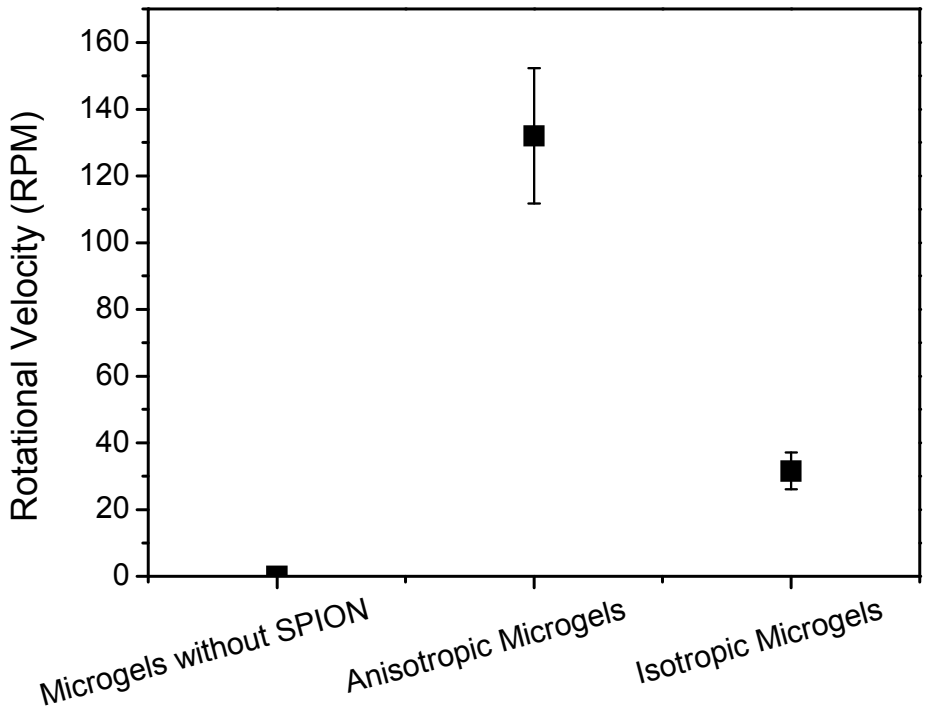

Fig. 5 Rotational velocity of microgels on a magnetic stirrer.

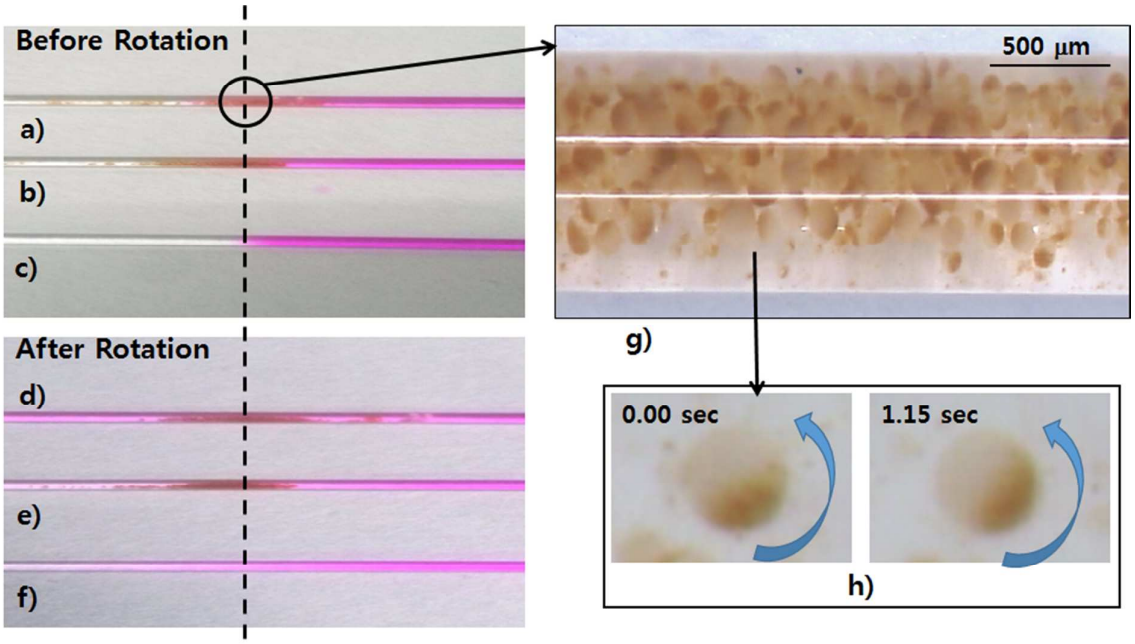

Fig. 6 Diffusion of rodamine-B (initially a 0.01 wt% aq. solution in the right part) in a capillary from right to left due to rotating microgels: a) anisotropic microgel, b) isotropic microgel, (c) no microgel, (d) anisotropic microgel under rotational magnetic field, e) isotropic microgel under rotational magnetic field, f) no microgel under rotational magnetic field, g) stereomicroscopic images of anisotropic particles inside the microcapillary, h) rotation of a single anisotropic microgel under rotational magnetic field (left: taken at 0 sec, right: taken at 1.15 sec later).

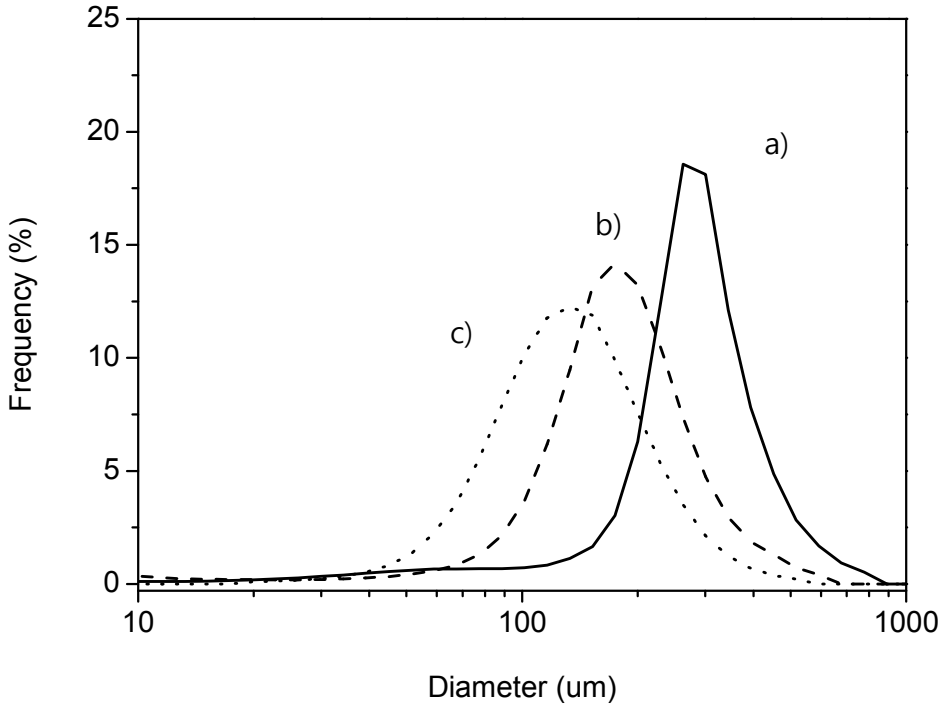

1

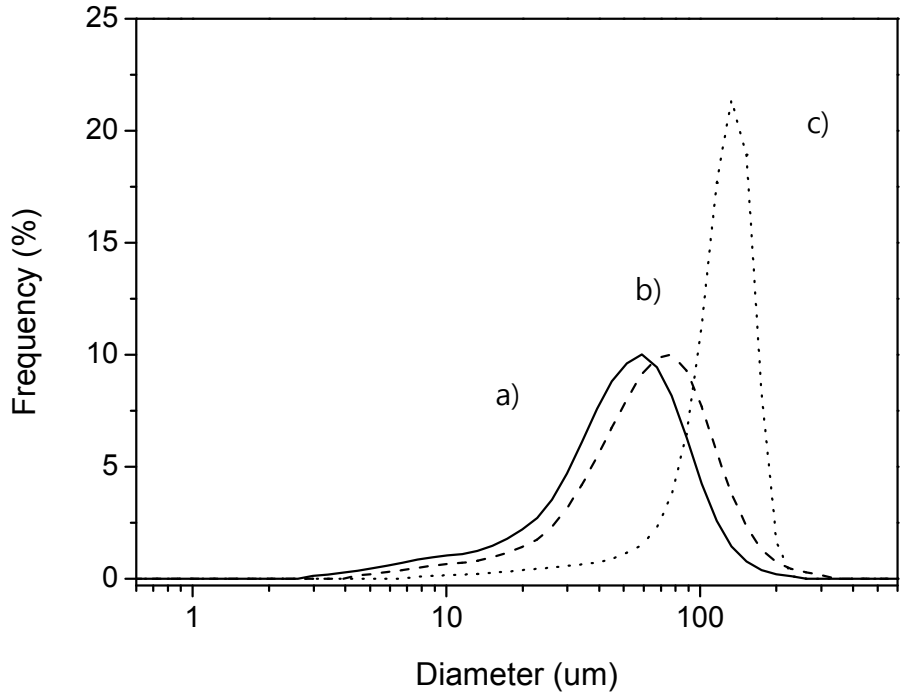

2
3

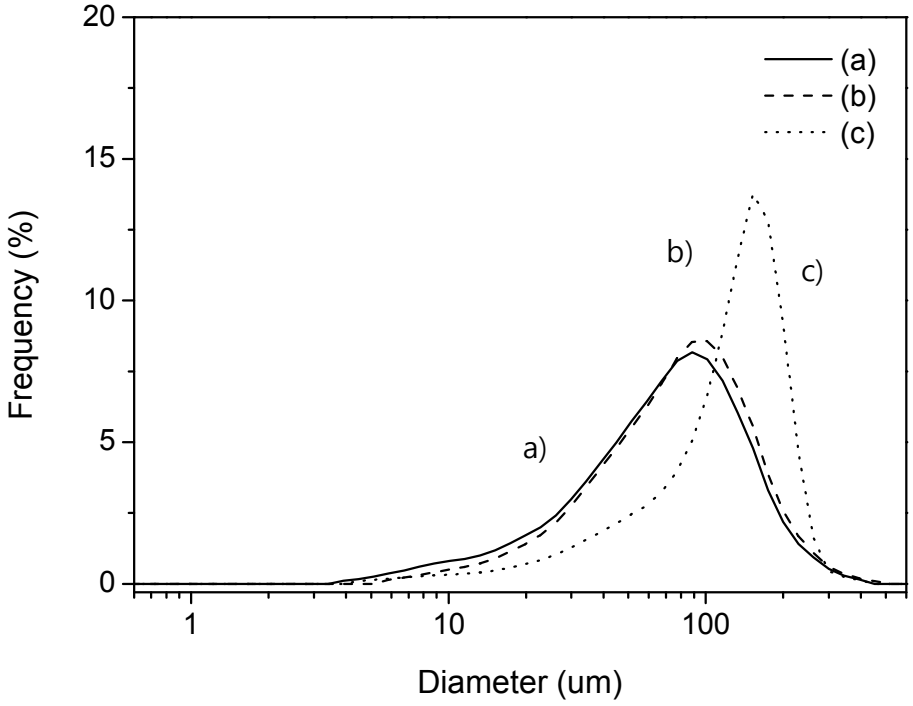

Fig. 7 Particle size analysis of microgels in water (top), pH 2 (middle) and pH 7 (bottom) buffer solutions as a function of SPION concentration in the monomer/SPION mixtures before crosslinking: (a) 1.45, (b) 0.73, (c) 0.36 wt%.

References

1. J. E. Herbert-Read, A. Perna, R. P. Mann, T. M. Schaerf, D. J. Sumpter and A. J. Ward, *Proceedings of the National Academy of Sciences*, 2011, **108**, 18726-18731.
2. N. Miller and R. Gerlai, *PloS one*, 2012, **7**, e48865.
3. R. W. Whittlesey, S. Liska and J. O. Dabiri, *Bioinspiration & Biomimetics*, 2010, **5**, 035005.
4. J. C. Liao, D. N. Beal, G. V. Lauder and M. S. Triantafyllou, *Science*, 2003, **302**, 1566-1569.
5. C. H. Ryer and B. L. Olla, *Marine Ecology Progress Series*, 1998, **167**, 215-226.
6. W. Sheng, O. O. Ogunwobi, T. Chen, J. Zhang, T. J. George, C. Liu and Z. H. Fan, *Lab on a Chip*, 2014, **14**, 89-98.
7. H. A. Stone, A. D. Stroock and A. Ajdari, *Annu. Rev. Fluid Mech.*, 2004, **36**, 381-411.
8. Y. Murakami, K. Araki, R. Ohashi, H. Honma, N. Misawa, K. Takahashi, K. Sawada and M. Ishida, *Sensors and Actuators B: Chemical*, 2014, **194**, 528-533.
9. C.-C. Chang and R.-J. Yang, *Microfluidics and Nanofluidics*, 2007, **3**, 501-525.
10. R. H. Liu, M. A. Stremler, K. V. Sharp, M. G. Olsen, J. G. Santiago, R. J. Adrian, H. Aref and D. J. Beebe, *Microelectromechanical Systems, Journal of*, 2000, **9**, 190-197.
11. J. Friend and L. Y. Yeo, *Reviews of Modern Physics*, 2011, **83**, 647.
12. L.-H. Lu, K. S. Ryu and C. Liu, *Microelectromechanical Systems, Journal of*, 2002, **11**, 462-469.
13. J. den Toonder, F. Bos, D. Broer, L. Filippini, M. Gillies, J. de Goede, T. Mol, M. Reijme, W. Talen and H. Wilderbeek, *Lab on a Chip*, 2008, **8**, 533-541.
14. A. Tripathi, H. Shum and A. C. Balazs, *Soft Matter*, 2014, **10**, 1416-1427.
15. G. Wang, Y. Zhang, Y. Fang and Z. Gu, *Journal of the American Ceramic Society*, 2007, **90**, 2067-2072.
16. J. Rubio-Retama, N. E. Zafeiropoulos, C. Serafinelli, R. Rojas-Reyna, B. Voit, E. Lopez Cabarcos and M. Stamm, *Langmuir*, 2007, **23**, 10280-10285.
17. J. K. Oh and J. M. Park, *Progress in Polymer Science*, 2011, **36**, 168-189.
18. H. Y. Koo, S. T. Chang, W. S. Choi, J.-H. Park, D.-Y. Kim and O. D. Velev, *Chemistry of Materials*, 2006, **18**, 3308-3313.
19. A. C. Siegel, S. S. Shevkoplyas, D. B. Weibel, D. A. Bruzewicz, A. W. Martinez and G. M. Whitesides, *Angewandte Chemie*, 2006, **118**, 7031-7036.
20. S. H. Kim, J. Y. Sim, J. M. Lim and S. M. Yang, *Angewandte Chemie*, 2010, **122**, 3874-3878.
21. Q. Gao, C. Wang, H. Liu, C. Wang, X. Liu and Z. Tong, *Polymer*, 2009, **50**, 2587-2594.
22. S. Lee, H. J. Kim, S. H. Chang and J. Lee, *Soft Matter*, 2013, **9**, 472-479.
23. N. Gundogan, O. Okay and W. Oppermann, *Macromolecular Chemistry and Physics*, 2004, **205**, 814-823.
24. S. Jin, M. Liu, F. Zhang, S. Chen and A. Niu, *Polymer*, 2006, **47**, 1526-1532.
25. N.-T. Nguyen, *Microfluidics and Nanofluidics*, 2012, **12**, 1-16.
26. G. K. Batchelor, *An Introduction to Fluid Dynamics*, Cambridge University Press, 2000.

27. C. H. Park and J. Lee, *Macromolecular Materials and Engineering*, 2010, **295**, 544-550.
28. D. Liu, W. Wu, J. Ling, S. Wen, N. Gu and X. Zhang, *Advanced Functional Materials*, 2011, **21**, 1498-1504.
29. J.-H. Ke, J.-J. Lin, J. R. Carey, J.-S. Chen, C.-Y. Chen and L.-F. Wang, *Biomaterials*, 2010, **31**, 1707-1715.
30. L. Zhou, B. He and F. Zhang, *ACS Applied Materials & Interfaces*, 2011, **4**, 192-199.
31. G. R. Bardajee, Z. Hooshyar and F. Rastgo, *Colloid and Polymer Science*, 2013, **291**, 2791-2803.